Isolated short attosecond pulse generated using a two-color laser and a high-order pulse

Hongchuan Du,[1] Huiqiao Wang,[2] and Bitao Hu[1,*]

[1]*School of Nuclear Science and Technology, Lanzhou University, Lanzhou 730000, China*

[2]*Institute of Theoretical Physics, Lanzhou University, Lanzhou 730000, China*

(Received 11 March 2010; published 15 June 2010)

An efficient method to generate an isolated short attosecond pulse is investigated theoretically. A broadband extreme ultraviolet supercontinuum harmonics can be generated when a model He^+ ion is exposed to the combination of an intense few-cycle laser pulse and a low-frequency field. By properly adding a 27th harmonics pulse to resonantly excite the He^+ ion, the intensity of the high-order harmonic generation (HHG) plateau is enhanced by 3–4 orders of magnitude. As a result, an isolated 24-as pulse with a bandwidth of 138 eV can be obtained directly from the supercontinuum around the cutoff of HHG.

DOI: 10.1103/PhysRevA.81.063813 PACS number(s): 42.65.Ky, 32.80.Rm, 42.65.Re

I. INTRODUCTION

The appearance and development of isolated attosecond pulses provide a means for probing and measuring basic ultrafast electronic processes, e.g., inner-shell electronic dynamics in atoms and molecules [1–4]. Because the HHG is a unique way to produce attosecond pulses in experiments, the attosecond pulse generation based on HHG has attracted a lot of attention. HHG processes can be well understood by the three-step model [5]. First the electron tunnels through the barrier formed by the Coulomb potential and the laser field, then it oscillates quasifreely driven by the laser field and acquires additional kinetic energy, and finally it can recombine with the parent ion. During recombination, a photon is emitted with the maximum photon energy given by $E_{\text{cutoff}}\,[\text{eV}] = I_p + 3.17U_p$, where I_p is the ionization potential of the atom and $U_p\,[\text{eV}] = 9.38 \times 10^{-14} I\,[\text{W/cm}^2]\,(\lambda_0\,[\mu\text{m}])^2$ is the ponderomotive energy of the electron in the laser field. This equation implies the harmonics spectrum has a sharp cutoff around the harmonics energy E_{cutoff}. After spectral filtering of the harmonic spectra at the plateau or cutoff region, a train of attosecond pulses could be produced. It has been demonstrated experimentally that attosecond pulse trains (APTs) [1] with duration of 250 as can be achieved by filtering HHG spectra. But for practical application, an isolated attosecond pulse is more useful, so much effort has been paid to extracting a single attosecond pulse. Isolated attosecond pulses with durations of 80 as [6] have been realized experimentally by filtering HHG spectra. However, the pulse is still significantly longer than 1 atomic unit of time (the atomic unit of time is 24 as), which is the time scale of electron motion in atoms. It has been suggested that the bandwidth of the attosecond pulse is more important than the duration in attosecond science [7]. So many efforts are underway to broaden the bandwidth of the attosecond pulse and push the duration to an even shorter time [8–11]. Very recently, an isolated sub-30-as pulse with the bandwidth of 170.5 eV [12] was realized theoretically. However, it may not be easy to realize such a large chirped laser pulse in actual experimental conditions.

In this paper, we propose a method for broadband xuv supercontinuum harmonic generation. The combination of a phase-stabilized few-cycle driving laser pulse and a low-frequency field is adopted. The harmonic spectrum is significantly extended to $I_p + 7.6U_p$ and the harmonics higher than $I_p + 4.8U_p$ are almost synchronically emitted for once. But the harmonic intensity is extremely low. By properly adding a 27th harmonics pulse, the intensity of HHG plateau is enhanced by 3–4 orders of magnitude. As a result, an isolated 24-as pulse with a bandwidth of 138 eV can be obtained directly from the supercontinuum around the cutoff of HHG.

II. THEORETICAL METHODS

The harmonics and the attosecond pulse generation can be studied by numerically solving the one-dimensional time-dependent Schrödinger equation. In our calculation, the soft Coulomb potential [13] $V(x) = -Z/\sqrt{a + x^2}$ is chosen with $Z = 2$ and $a = 0.5$ to match the ionization potential $E_0 = -2.0$ a.u. of a real He^+ ion. The electric field of the driving laser can be expressed as

$$E(t) = E_0 f_0(t) \cos[\omega_0(t - \tau) + \phi_{\text{CEP}}] + E_1 \sin(\omega_1 t). \quad (1)$$

Here τ is the time delay between the few-cycle pulse and the low-frequency field. E_i and ω_i $(i = 0,1)$ are the peak amplitudes and frequencies of the fundamental and low-frequency pulses, respectively. $f_0(t) = \sin^2(\pi t/T_0)$ presents the profile of the few-cycle laser field. ϕ_{CEP} is the carrier-envelope phase of the few-cycle driving pulse and is set as 0 through the paper.

The one-dimensional time-dependent Schrödinger equation is solved accurately and efficiently by means of the split-operator method [14]. Once the time evolution of the wave function $\psi(x,t)$ is determined, the time-dependent induced dipole acceleration can be given by means of Ehrenfest's theorem

$$a(t) = -\langle\psi(x,t)|\frac{\partial V(x)}{\partial x} - E(t)|\psi(x,t)\rangle. \quad (2)$$

The harmonic spectrum can be obtained, which is proportional to the modulus squared of the Fourier transform of $a(t)$,

$$P_A(\omega) = \left|\frac{1}{\sqrt{2\pi}}\int_0^{T_0} a(t)e^{-i\omega t}\,dt\right|^2. \quad (3)$$

*hubt@lzu.edu.cn

By superposing several orders of the harmonics, an ultrashort pulse can be obtained with the temporal profile

$$I(t) = \left| \sum_q a_q e^{i\omega t} \right|^2, \quad (4)$$

where $a_q = \int a(t) e^{-i\omega t} dt$.

III. RESULTS AND DISCUSSION

In order to demonstrate our scheme, we first investigate the HHG process in terms of the semiclassical three-step model, which presents a clear physical picture. In our calculation, $T_0 = 552$ a.u. corresponds to a duration of 5 fs full width at half maximum (FWHM). We choose $\omega_0 = 0.057$ a.u. and $\omega_1 = 0.0057$ a.u. corresponding to $\lambda_0 = 800$ nm and $\lambda_1 = 8$ μm, respectively. τ is set as $T_0/2$. The intensities of the driving and the control pulses are 0.24 and 0.1 a.u., respectively.

Figure 1 illustrates the sketch of the electron dynamics. In Fig. 1(a), the time varying of combined driving laser field is presented. The electron is ionized from $1.6T$ to $2.0T$ and from $2.6T$ to $3.0T$ ($T = 2\pi/\omega_0$ is an optical period of the few-cycle pulse) forming only two returns (marked as R1 and R2). In every optical cycle of the few-cycle pulse, the low-frequency field does not change its direction. In the half cycle of $t = 2.5T$, the total field is greatly enhanced and the electron accelerated here gains much more energy, therefore the harmonic spectrum can be significantly extended; i.e., the cutoff region is much higher than the well-known value of $I_p + 3.17U_p$. To substantiate such a fact, we analyze the dependence of the kinetic energy E_k on the ionization times t_i and emission times t_e. The result is shown in Fig. 1(b). There are two major emission events taking place, near the peaks labeled A and B. The maximum kinetic energy of R1

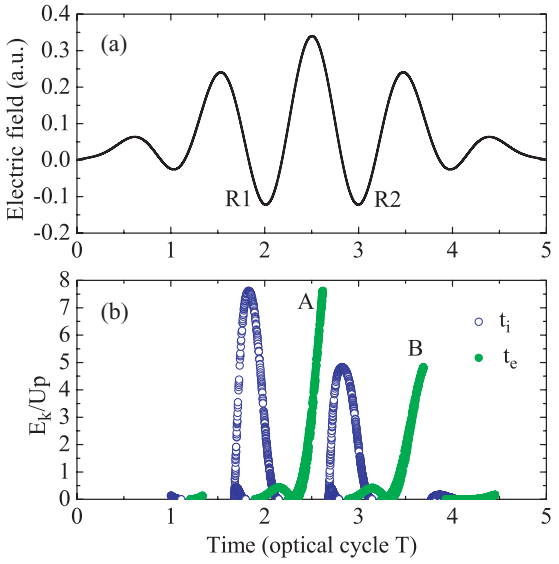

FIG. 1. (Color online) (a) Driving laser field of the fundamental laser ($\omega_0 = 0.057$ a.u.) in combination with a low-frequency field ($\omega_1 = 0.0057$ a.u.). (b) The dependence of the kinetic energy E_k on the ionization (unfilled blue circles) and recombination times (filled green circles). The intensities of the driving pulse and the low-frequency field are 0.24 and 0.1 a.u., respectively.

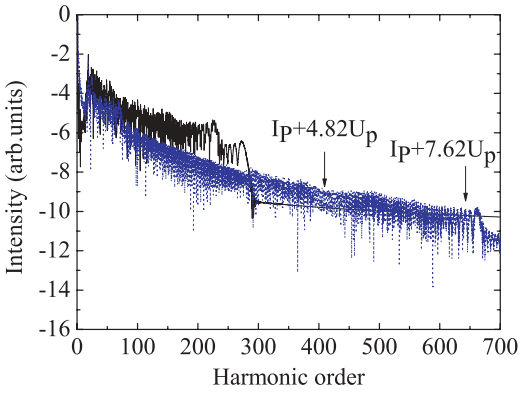

FIG. 2. (Color online) The HHG power spectra from the model He^+ ion in the fundamental field (solid black line), and in the fundamental laser in combination with a low-frequency field (dashed blue line). The same parameters as in Fig. 1.

reaches $7.62U_p$ ($U_p = E_0^2/4\omega_0^2$), while that of R2 only reaches $4.82U_p$. In the range of peak B, there are two dominant quantum paths with different emission times and the first plateau is formed. However, in the range of peak A, where the second plateau is formed, two dominant quantum paths have almost the same emission time. So we can conclude that under modulation of the low-frequency field, the HHG spectrum can be extended to $I_p + 7.62U_p$, and the harmonics higher than $I_p + 4.82U_p$ are almost locked in phase and emitted once, i.e., become supercontinuous, which results in a broad supercontinuum spectrum with the bandwidth of 338 eV.

Following, we perform the calculation to confirm the above classical approaches by numerically solving the time-dependent Schrödinger equation. The parameters are the same as those in Fig. 1. The harmonic spectrum is shown in Fig. 2. For comparison, the harmonic spectrum in the driving pulse alone is also given (solid black line). It is seen that the width of the HHG plateau for the case of adding a

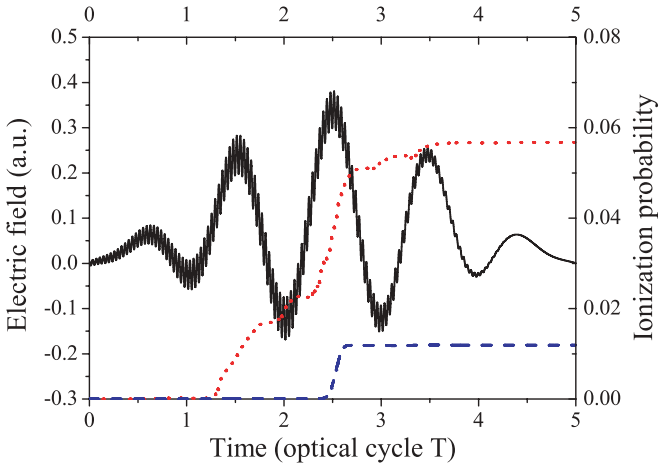

FIG. 3. (Color online) The electric field (solid black line) with the 27th harmonics pulses ($\omega\tau_{\text{delay}} = -1.09\pi$) and the dependence of the ionization probability on time without the 27th harmonics pulses (dash blue line) and with the 27th harmonics pulses (dotted red line). The 27th harmonics pulse intensity is 0.0463 a.u. and the other parameters are the same as in Fig. 1.

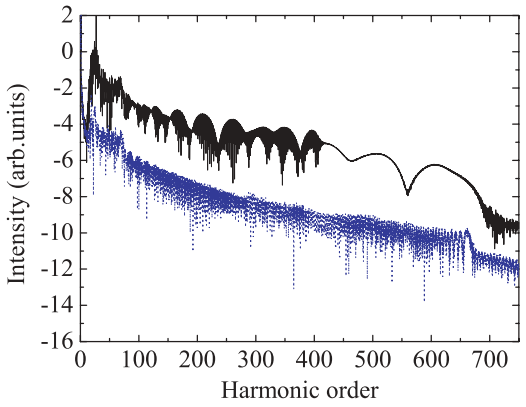

FIG. 4. (Color online) The HHG power spectra from model He^+ ion with the 27th harmonics pulses (solid black line) and without the 27th harmonics pulses (dotted blue line). The same parameters as in Fig. 3.

low-frequency laser pulse is significantly extended compared with the case of the fundamental laser alone. But the harmonic intensity is extremely low. According to the three-step model, the harmonic efficiency is mainly laid on the ionization rate. In order to enhance the conversion efficiency, a 27th harmonics pulse ($\omega\tau_{\text{delay}} = -1.09\pi$) is superposed to Eq. (1). The harmonics pulse intensity is set as 0.0463 a.u. For our model He^+ ion, the 27th harmonics pulse promotes a resonant transition from the ground state to the second exited states [12] and enhances the ionization probability of He^+. The time variance of the combined driving laser field is presented in Fig. 3. The ionization probability is also shown in Fig. 3. In our scheme, the continuous harmonics mainly originate from the electrons ionized in the time range from $1.6T$ to $2.0T$. Since the ionization probability of adding a 27th harmonics pulse (dotted red curve) is larger than that (dash blue curve) without adding it in the time range, the efficiency of the continuous harmonics will be enhanced by adding a 27th harmonics pulse.

Figure 4 shows the harmonic spectrum for the case. The harmonic spectrum in the synthesized two-color pulse alone is also presented for comparison (dotted blue curve). As shown in this figure, the intensity of the broadband supercontinuum is greatly enhanced by 3 or 4 orders and is comparable with

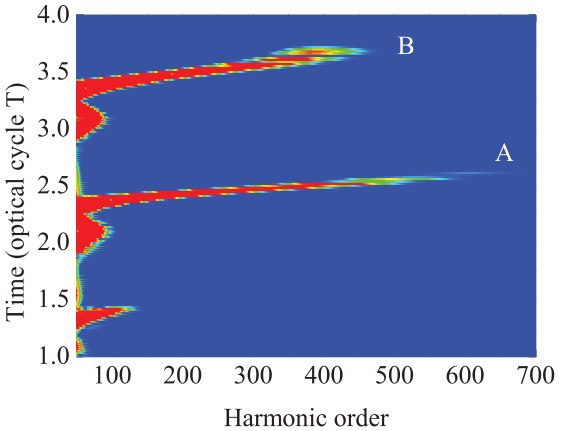

FIG. 5. (Color online) Wavelet time-frequency profile of HHG power spectra from 50 to 700 corresponding to the solid line in Fig. 4.

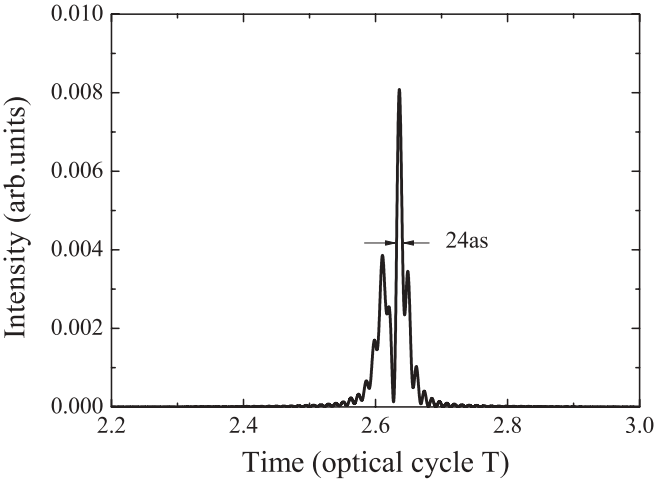

FIG. 6. The temporal profile of the isolated attosecond pulse by superposing the harmonics from 528 to 616. The same parameters as in Fig. 3.

that of the lower irregular harmonics. One can also see that the interference structure of the harmonic spectrum changes when the harmonic pulse is existent. It is different with those reported in Refs. [15,16]. In their scheme, the controlling attosecond pulse train can put an electron into continuum with $v > 0$, which leads to the different spectrum structure. In this paper, the motivation of using the 27th harmonics pulse is a resonant transition from the ground state to the second exited states, not to the continuum states. Then the two-color pulse can easily ionize the ion from the second exited states. In our situation, the change of the interference structure is due to quantum path selection. Because the ionization potential of the He^+ ion is large, and the effective ionization takes place where the electric field is close to zero, the quantum paths A and B are very weak. When the harmonic pulse is added, the effective ionization is enhanced, which leads to the quantum paths A and B dominating. The time-frequency distribution [17] is presented to further understand the harmonic spectrum, which is shown in Fig. 5. As shown in this figure, there are two main

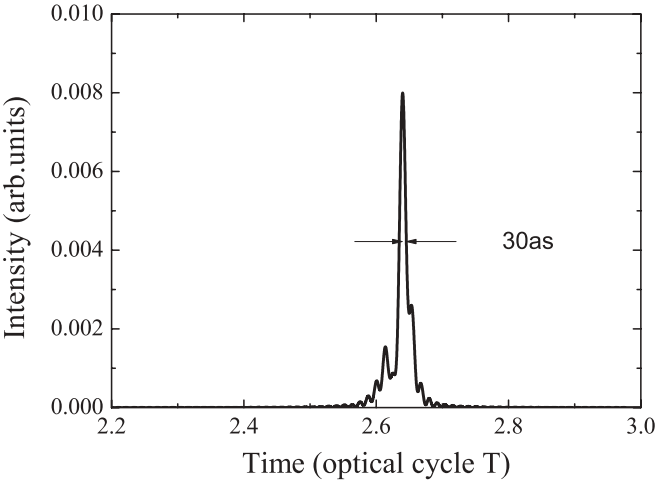

FIG. 7. The temporal profile of the isolated attosecond pulse by superposing the harmonics from 538 to 622. The same parameters as in Fig. 3.

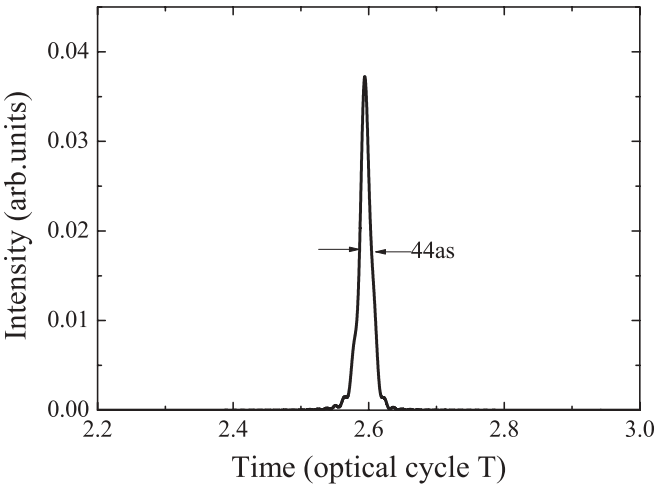

FIG. 8. The temporal profile of the isolated attosecond pulse by superposing the harmonics from 460 to 540. The same parameters as in Fig. 3.

peaks contributing to the harmonics (marked A and B). Each burst emission time agrees remarkably well with the classical recollision time shown in Fig. 1(b). The contribution of those two quantum paths in the range of peak A is nearly the same. Around the range of peak B, the two quantum paths join each other.

When only a single quantum path contributes to the HHG, a very short attosecond pulse can be obtained directly by superposing several harmonics which have almost the same emission time. Figure 6 shows the time profile of the generated isolated attosecond pulse. When we select 89 harmonics (from 528 to 616), as shown in Fig. 6, the duration of this isolated attosecond pulse is about 24 as (FWHM) with a bandwidth of 138 eV, which is first equal to 1 atomic unit of time (24 as) by straightforward filtering of the HHG spectrum. Such a short isolated attosecond pulse will enable the detection and control of the electronic dynamics inside atoms and molecules.

The different ultrashort isolated attosecond pulses can be obtained by superposing different harmonics. Figure 7 shows the time profile of the generated isolated attosecond pulse via superposing 85 order harmonics (from 538 to 622). A 30-as clean isolated short attosecond pulse with a bandwidth of 131.8 eV is produced. Figure 8 shows the time profile of the generated isolated attosecond pulse via superposing 81 order harmonics (from 460 to 540). It can be seen that a 44-as clean isolated pulse with a bandwidth of 125.6 eV is generated.

IV. CONCLUSION

In conclusion, we present an efficient method to generate broadband extreme ultraviolet supercontinuum harmonics via a model He^+ ion exposed in a combined field of an intense few-cycle laser and a low-frequency field. It is achieved by significantly modulating the quantum paths of HHG. The harmonic spectrum can be extended to $I_p + 7.62U_p$ and the harmonics higher than $I_p + 4.82U_p$ are almost synchronically emitted for once, which results in an xuv supercontinuum with the bandwidth of $2.8U_p$. By adding a 27th harmonics pulse to resonantly excite the He^+ ion, the intensity of the HHG plateau is enhanced by 3–4 orders of magnitude when adopting the proper time delay between the harmonic pulse and the fundamental laser. In this case, the generation of the isolated attosecond pulses is also investigated. An isolated attosecond pulse with a duration of 24 as can be obtained directly which is first equal to 1 atomic unit of time (24 as) by straightforwardly filtering the HHG spectrum. Such a short isolated attosecond pulse will enable the probing and monitoring electron dynamics deep inside atoms and molecules.

ACKNOWLEDGMENTS

We thank Dr. Weiyi Hong in Huazhong University of Science and Technology for helpful discussions. This work was supported by the Program for New Century Excellent Talents in University and the National Natural Science Foundation of China under Grant Nos. 10775062 and 10875054.

[1] P. M. Paul *et al.*, Science **292**, 1689 (2001).
[2] R. Kienberger *et al.*, Nature (London) **427**, 817 (2004).
[3] K. J. Schafer, M. B. Gaarde, A. Heinrich, J. Biegert, and U. Keller, Phys. Rev. Lett. **92**, 023003 (2004).
[4] P. Johnsson *et al.*, Phys. Rev. Lett. **95**, 013001 (2005).
[5] P. B. Corkum, Phys. Rev. Lett. **71**, 1994 (1993).
[6] E. Goulielmakis *et al.*, Science **320**, 1614 (2008).
[7] P. Lan, P. Lu, W. Cao, Y. Li, and X. Wang, Phys. Rev. A **76**, 011402(R) (2007).
[8] Weiyi Hong, Peixiang Lu, Pengfei Lan, Zhenyu Yang, Yuhua Li, and Qing Liao, Phys. Rev. A **77**, 033410 (2008).
[9] Weiyi Hong, Peixiang Lu, Wei Cao, Pengfei Lan, and Xinlin Wang, J. Phys. B **40**, 2321 (2007).
[10] Weiyi Hong, Qingbin Zhang, Zhenyu Yang, and Peixiang Lu, Phys. Rev. A **80**, 053407 (2009).
[11] Zhinan Zeng, Ya Cheng, Xiaohong Song, Ruxin Li, and Zhizhan Xu, Phys. Rev. Lett. **98**, 203901 (2007).
[12] Peng-Cheng Li, Xiao-Xin Zhou, Guo-Li Wang, and Zeng-Xiu Zhao, Phys. Rev. A **80**, 053825 (2009).
[13] J. Javanainen, J. H. Eberly, and Q. Su, Phys. Rev. A **38**, 3430 (1988).
[14] N. Watanabe and M. Tsukada, Phys. Rev. E **62**, 2914 (2000).
[15] A. Bandrauk and N. Shon, Phys. Rev. A **66**, 031401(R) (2002).
[16] C. Figueira de Morisson Faria, P. Salieres, P. Villain, and M. Lewenstein, Phys. Rev. A **74**, 053416 (2006).
[17] P. Antoine, B. Piraux, and A. Maquet, Phys. Rev. A **51**, R1750 (1995).